ASRL TR 1008

VELOCITY CORRELATION MEASUREMENTS IN THE MIXING REGION OF A JET

MARC A. KOLPIN

OTS PRICE

XEROX $ [redacted]

MICROFILM $

MASSACHUSETTS INSTITUTE OF TECHNOLOGY

AEROELASTIC AND STRUCTURES RESEARCH LABORATORY

MARCH 1963

Code 1

COPY

VELOCITY CORRELATION MEASUREMENTS IN THE MIXING REGION OF A JET

by
M. A. Kolpin

Department of Aeronautics and Astronautics
Massachusetts Institute of Technology

SUMMARY

/ 6683

Measurements of space-time correlations of the u-component of turbulence in the mixing region of a jet are presented. It is shown that the longitudinal correlation function

$$R = \frac{\langle u(x,t)\; u(x+\Delta x, t+\tau)\rangle}{u'(x,t)\; u'(x+\Delta x, t+\tau)}$$

depends only upon the nondimensional quantities

$$\tau^* = \frac{\tau U_{exit}}{x} \qquad \frac{\Delta \xi}{\xi} \qquad \text{where} \quad \xi = \frac{x}{d}$$

On the cylinder $r = d/2$ the convection speed of the turbulent field was different for the different eddy sizes, varying from the local mean-speed for small eddies to $1/2\, U_{exit}$ for the large eddies.

The lateral correlation function for zero time delay is shown to be of the form $R_\eta = R_\eta\left(\frac{\Delta\eta}{\xi}\right)$ where $\eta = \frac{r - d/2}{x}$ and is monotonically decaying with increased wire separation.

Measurements of the angular correlation function are reported which show no correlation of the fluctuations across the diameter of the jet.

VELOCITY CORRELATION MEASUREMENTS IN THE MIXING REGION OF A JET

1. Introduction

The correlation measurements reported here are fragmentary results of a broad experimental investigation of jet flows and jet noise currently under way at the Massachusetts Institute of Technology. A more detailed paper discussing these and other results has been submitted for publication. Measurements of mean Mach number and temperature profiles along with the measurement of turbulence intensity and power spectra led us to believe that the following dimensionless quantities were relevant when analyzing the structure of the turbulent field in the mixing region of a jet.

conical coordinate $\eta = \frac{r - d/2}{x}$

delay time $\tau^* = \frac{\tau U_{exit}}{x}$

correlation length $\xi^* = \frac{\Delta \xi}{\xi}$

It will be our thesis that these dimensionless quantities can be shown experimentally to be adequate to describe the space-time correlation of the u-component of turbulence in the early shear layer of a jet.

2. Experimental arrangement

The flow producing system was the same as described by Mollö-Christensen in a previous paper in this series. The traversing mechanism for the hot-wire probes shown in Fig. 1 was

of a design permitting the free and independent motion of the probes along the three cylindrical coordinates x, r, and θ. The alignment of the traversing mechanism was achieved by recording profiles of total pressure. The hot-wires, while in operation, could be observed through a microscope and vibrations thus be detected and eliminated. The microscope also helped to relocate the probes after a wire failure. Repeatability of position was within ± 0.0025 cm. The constant current hot-wire sets used in this investigation are commercially available and are manufactured by Shapiro and Edwards, South Pasadena, California. The input circuit noise was chopped off at 80 kc. when the amplifiers were compensated. The reader is referred to the paper by Mollo-Christensen for a description of the automatic recording correlation computer. (Fig. 2.)

2.1 Coordinate system and nomenclature

A cylindrical coordinate system is used to describe the measurements. The x-coordinate is measured along the jet axis, the r-coordinate being perpendicular to it. The data are plotted in terms of the nondimensional variables $\xi = \frac{x}{d}$ and $\eta = \frac{r - d/2}{x}$ where d is the jet diameter. The wire separations in the correlation measurements are expressed as

$$\Delta\xi = \frac{\Delta x}{d}, \quad \Delta\eta = \frac{\Delta r}{d}, \quad \Delta_\theta = \frac{r\Delta\theta}{d}.$$

The characteristic time is taken to be proportional to the local shear layer thickness. The reduced delay time then becomes $\tau^* = \frac{\tau U_{exit}}{x}$

Other notations are: Re, the Reynolds number based on jet diameter, M, the Mach number, U, the local mean velocity, u, the axial component of the turbulent velocity vector, u', the RMS of u. The subscript "exit" refers to conditions in the plane $x = 0$.

2.2 The domain of investigation

The physical dimensions of the shear flow under investigation being rather small, especially normal to the mean flow direction, it was not practical to study the v-component of the turbulent field with x-hot-wire probes. We shall then be concerned only with the u-component. Furthermore, our limited knowledge of the laws of heat transfer to thin wire in the range $0.5 < M \leq 1.2$ makes the calibration of the individual wires a very time consuming operation. When compared with the relatively short lifetime of the wire due to the high dynamic loading and dust particles' impact, a good operating range of M_{exit} was found to be $M_{exit} < .5$.

3. Correlation measurements

The two-point longitudinal correlation or covariance of the u-component of the velocity fluctuation is defined as

$$R = \frac{\langle u(x,t)\, u(x+\Delta x, t+\tau)\rangle}{u'(x,t)\; u'(x+\Delta x, t+\tau)}$$

We shall use the symbols R_E for the autocorrelation function

$$R_E = \frac{\langle u(x,t)\, u(x, t+\tau)\rangle}{u'(x,t)\; u'(x, t+\tau)}$$

and R_ξ, R_η, R_θ for the spatial correlation function with the wire separation in the x, r, and θ directions.

The autocorrelation function was measured for different ξ locations and its similarity investigated. Fig. 3 shows that, if the time delay τ is made dimensionless with respect to the local shear rate, similarity is quite apparent.

In Fig. 4 is reproduced R_ξ for different axial positions. If the wire separation is made dimensionless with a factor proportional to the local shear layer thickness, the similarity is obvious. Laurence's measurements of R_E and R_ξ agree very clearly with ours when expressed in terms of τ^* & $\frac{\Delta\xi}{\xi}$. Note that in both cases, the maximum negative value of the autocorrelation function increases with increasing ξ . We believe this to be caused not by a lack of similarity in the flow, but by the inadequate low-frequency cutoff of the correlation computer.

Before presenting some measured space-time correlation functions, let us discuss quantitatively possible interpretations of R in terms of the flow field. Fig. 5 shows four characteristic shapes of the correlation function.

(a) $R(\tau, \Delta\xi, \xi) = f_1(\tau - d U \Delta\xi)$

The turbulent pattern is totally frozen and is convected with the velocity U. By definition $f_1(0) = 1$.

(b) $R(\tau, \Delta\xi, \xi) = g_1(d \Delta\xi) f_1(\tau - d U \Delta\xi)$

where g_1 is a monotonically decreasing function with $g_1(0) = 1$. The convected turbulent pattern is only partially frozen. Between the two wires new eddies are

created from the old ones at a rate given by the decay of g_1. It is important to note that the rate of the formation is the same for all eddy sizes. The distance $d \Delta \xi$ for which g_1 is reduced by a half is the necessary distance to renew half the field. Case a) and b) imply also homogeneity of the field in the axial direction.

c) The apex of the correlation function is rounded while the rest of the curve remains almost unchanged during its translation along the axis. The small eddies have a much shorter lifetime than the large ones. They ride in a sense on a frozen pattern of large eddies.

d) From an even function, the correlation function becomes odd. Large disturbances are shed at random times and move slower than the convection speed.

Using these elementary patterns it is now possible to tentatively interpret the meaning of the measured space-time correlation function shown on Fig. 6, 7, and 8.

The turbulent field is convected with an average velocity of approximately 60 m/sec. which is also the mean velocity for $\eta = 0$. The short lifetime of the small eddies very rapidly rounds off the peak for $\tau^* \sim \frac{\Delta \xi}{\xi}$. As the wire separation gets larger, only disturbances of the order of magnitude of the shear layer width are correlated. The disturbances are now convected at half the

exit velocity, and the correlation function slowly changes to the odd shape.

In Fig. 9 is shown that indeed within experimental error, the space-time correlation function can be expressed in terms of the two dimensionless variables τ^{*} & ξ^{*} over a wide range of conditions.

Fig. 10 shows the decay rate of the various eddy size as seen by an observer riding with the flow. Their convection speed can also be read from this figure. These curves were obtained by filtering the hot-wire signals through two Krohn-Hite variable band pass filters before feeding them into the correlation computer. These measurements confirm our interpretation that the large eddies are convected slower $[U_{conv} = \frac{1}{2} U_{ex}]$ than the small one $[U_{conv} = U_{local}]$

In accordance with these measurements, we expect to be able to write for the lateral correlation function.

$$R_{\eta} = R_{\eta}\left(\frac{\Delta\eta}{\xi}\right)$$

This hypothesis is tested in Fig. 11a where it is shown to be true. The monotonic decay of the function with increasing $\Delta\eta$ indicates that the shear layer as a whole has no instability mode of finite amplitude.

We also investigated the possible feed-back influence of the annular shear layer on itself through the laminar core. Space-

time correlation curves were recorded for the wires located at different angular position in the plane $\xi = 3$.

Fig.11b indicates that there is no feed-back across the laminar core. The correlation curve shows only the three dimensional character of turbulence.

4. Conclusion

We have reported some measurements of the space-time correlation function of the u-component of the turbulent field in the mixing region of a jet. We have shown that the correlation function can be represented in the form $R = R(\tau^*, \xi^*)$. The volume over which the velocity fluctuations are correlated is of primary importance if the sound field emitted by the turbulent flow is to be computed. We are now in a position to determine the correlation volume by looking at the three dimensional plot of the space-time correlation function.

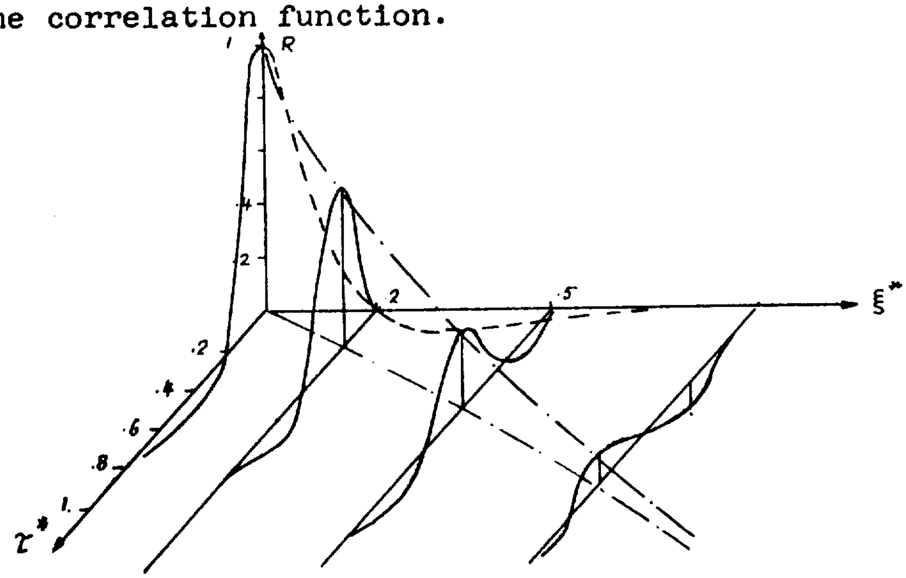

We can see that the correlated volume has a length in the flow direction of approximately $1.6\,\xi$ and extends upstream and downstream of the fixed point. The lateral and angular extent of the volume can be deduced from the lateral and angular correlation curve. It is of order of magnitude δ in both directions. The sound field emitted by each of the correlation volume being uncorrelated, they can be studied separately and, then, superimposed linearly.

This work was supported by the National Aeronautics & Space Administration under Grant NsG 31-60.

Reference:

Laurence, J. C. Intensity, Scale & Spectra of Turbulence in Mixing of Free Subsonic Jet, NACA TR 1292, April 1956.

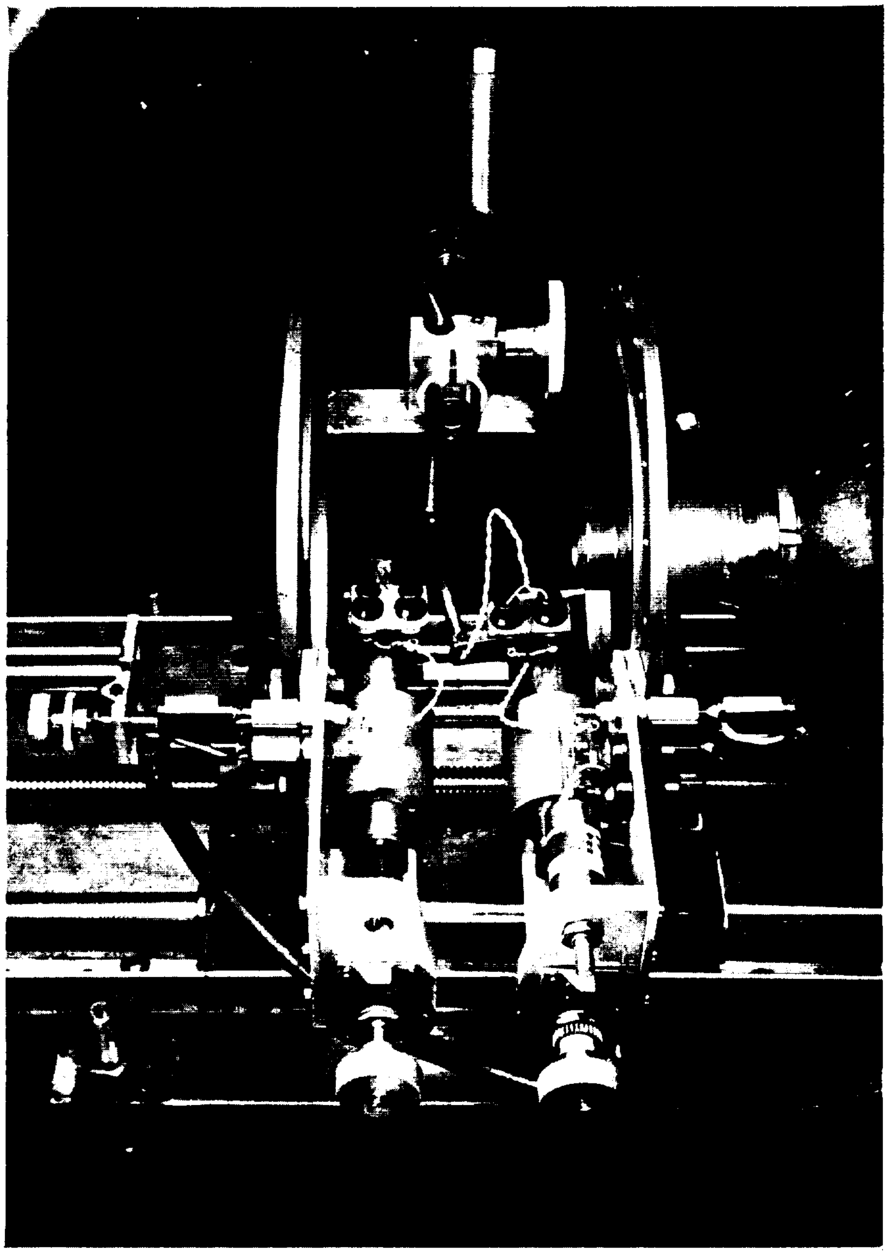

Figure 1 Probe Configuration for Space-Time Correlation Measurements

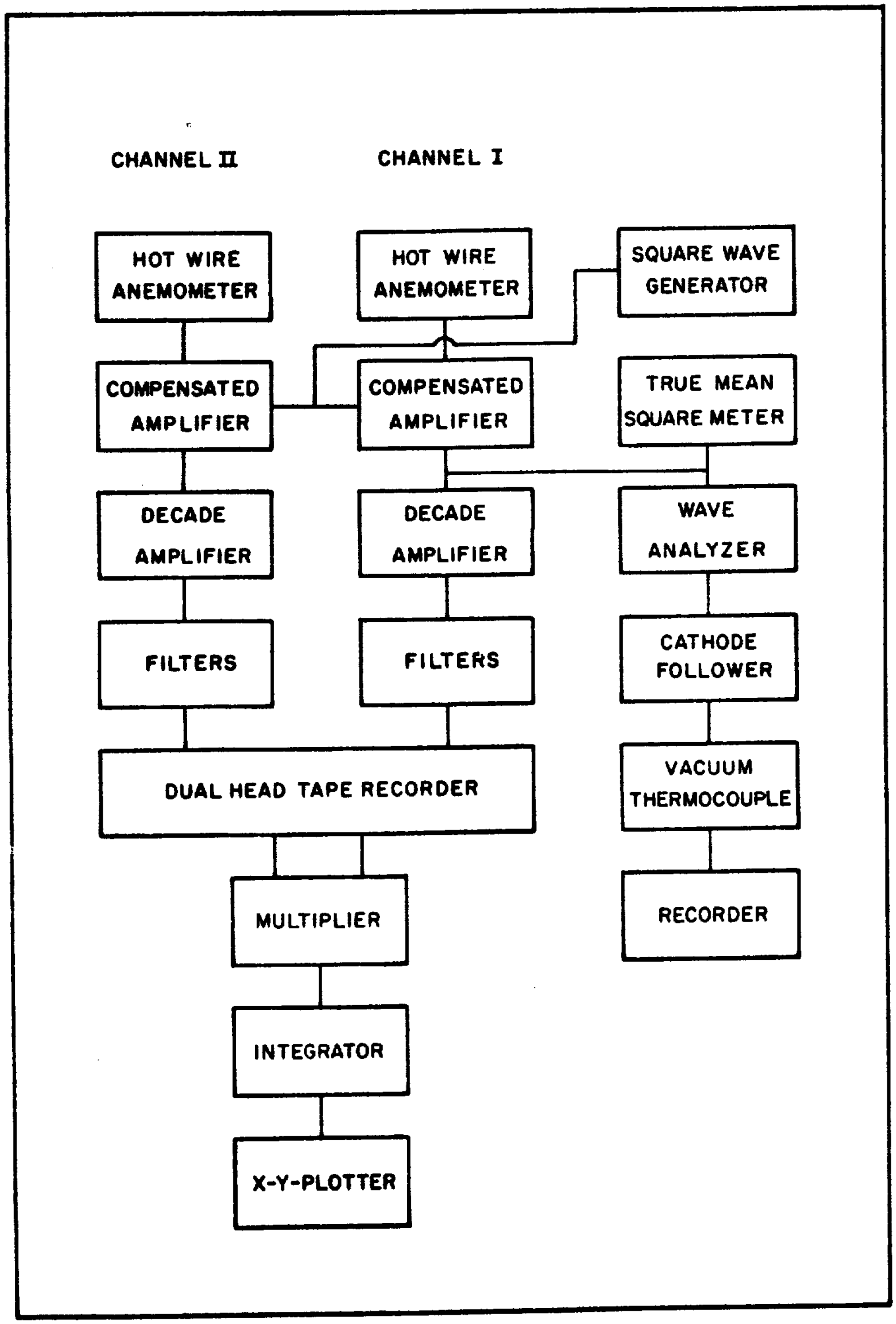

Figure 2 Block Diagram of the Analogue Data Recording System for the Hot Wire Measurements

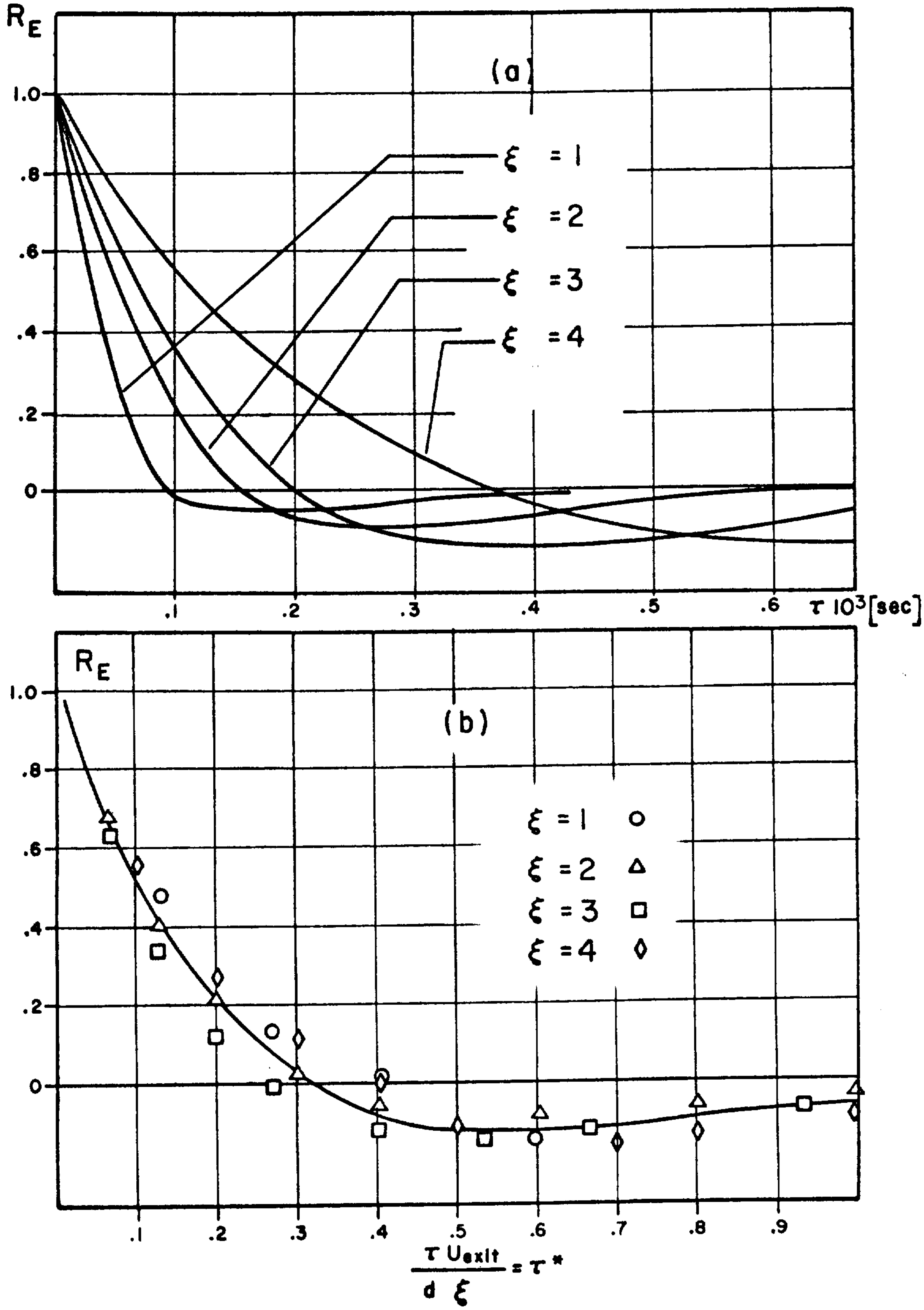

Figure 3 Autocorrelation Coefficient $M_{ex} = 0.3$, d = 1"
(a) Axial Development (b) Similarity

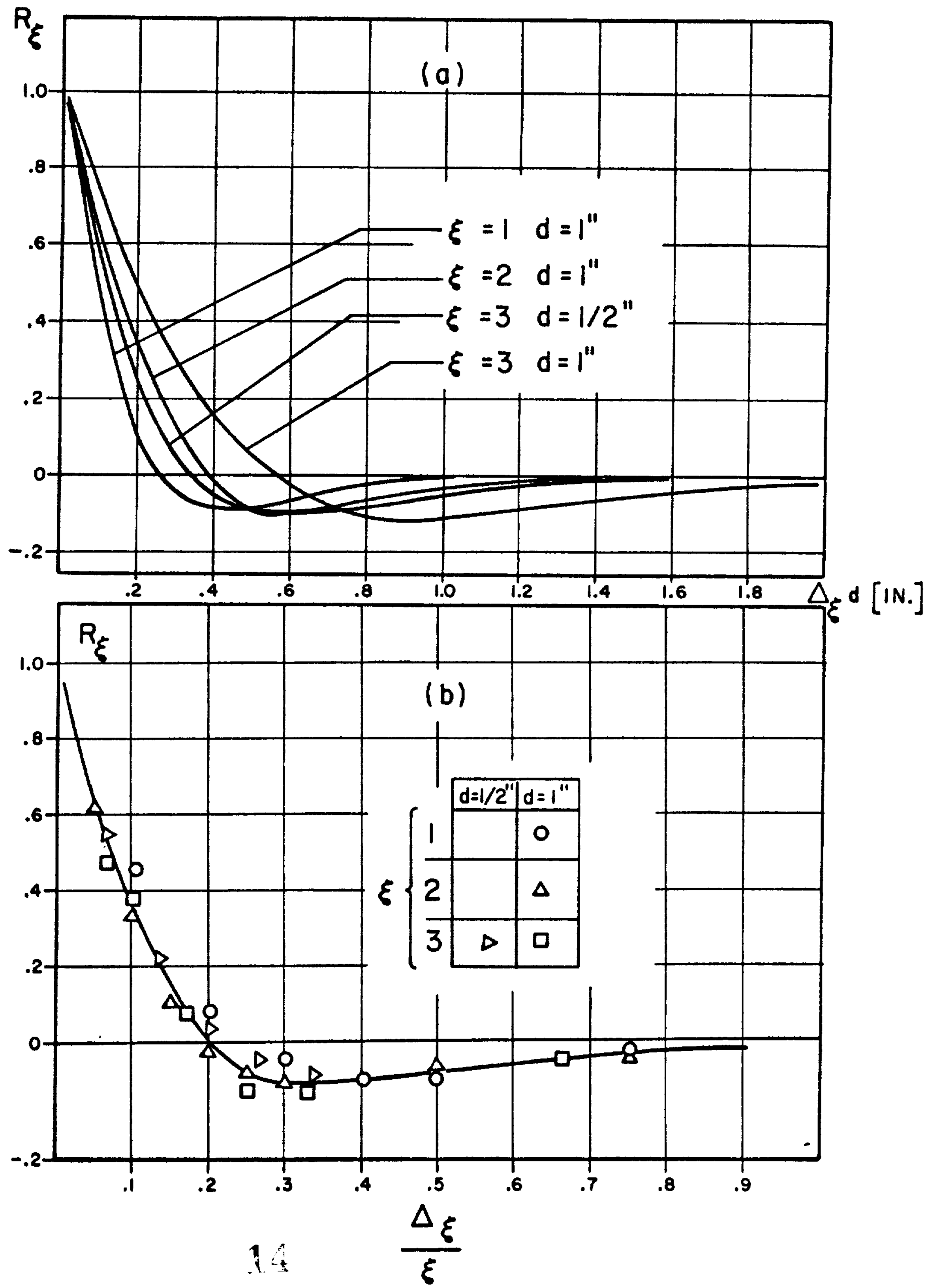

14

Figure 4 Longitudinal Correlation Coefficient. M_{ex} = 0.3
(a) Axial Development (b) Similarity

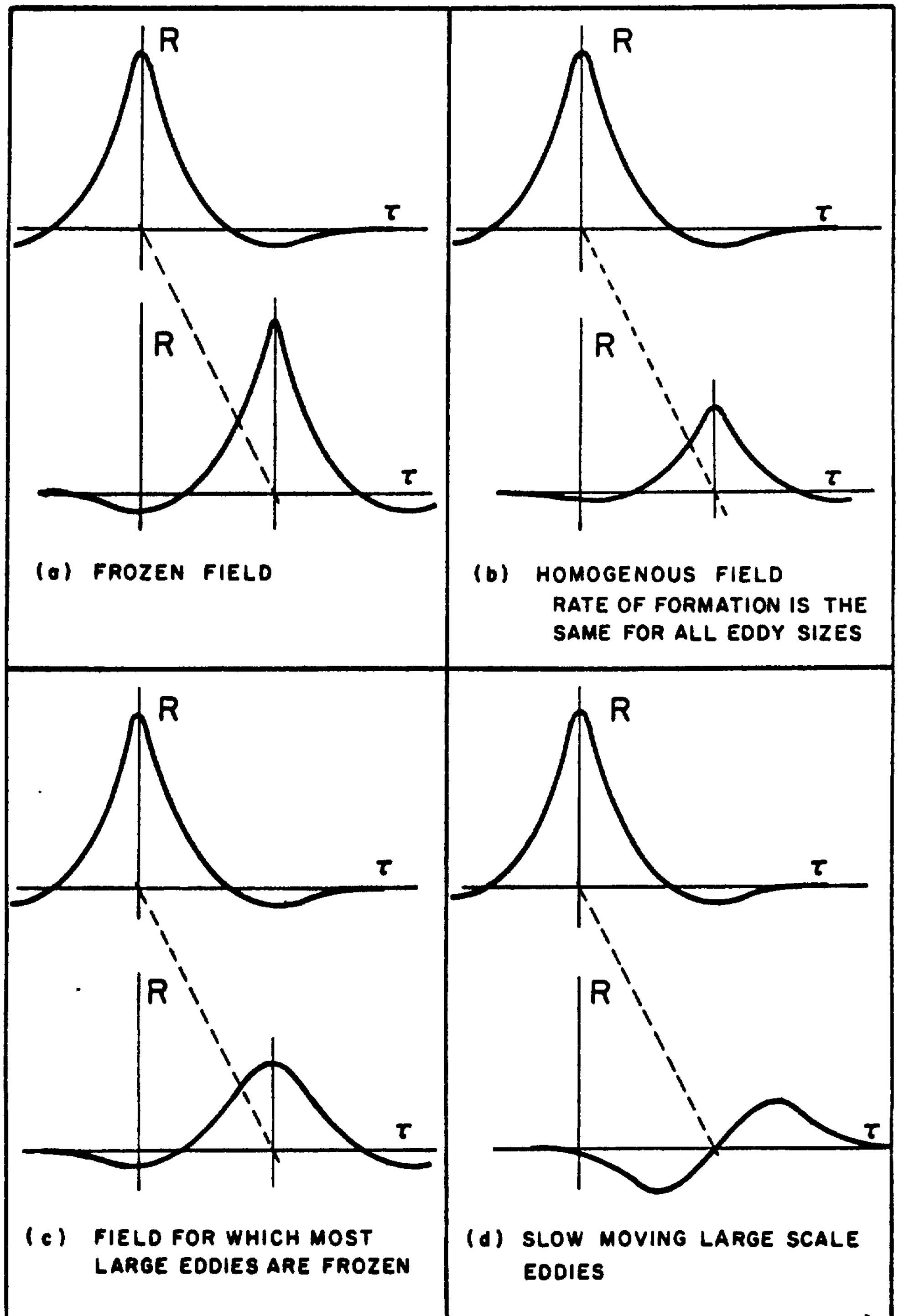

Figure 5 Characteristic Cross-correlation Functions for some Hypothetical Turbulence Patterns.

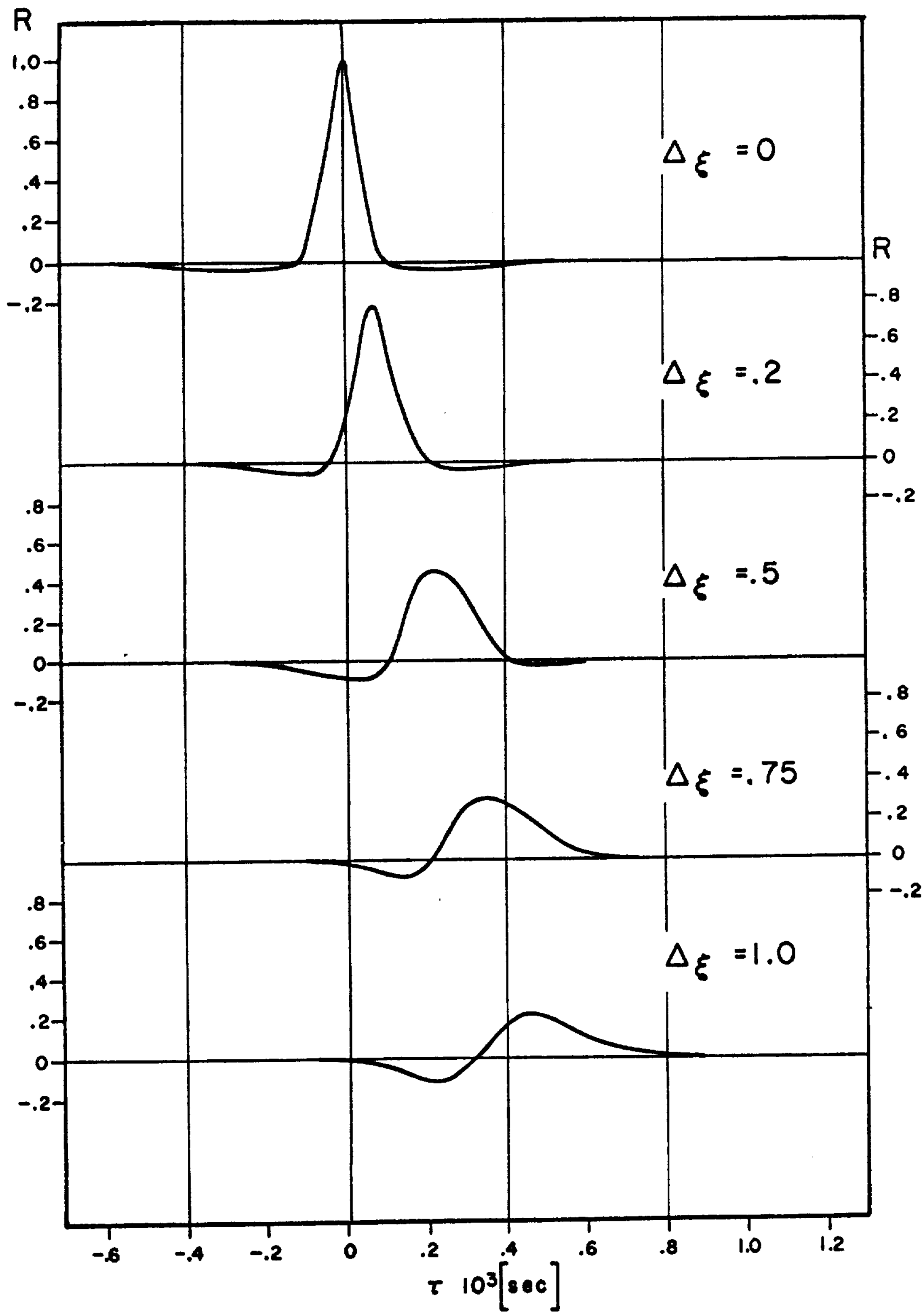

Figure 6 Space-time Correlation Coefficient
$\xi = 1$, $M_{ex} = .3$, $\eta = 0$, $d = 1''$

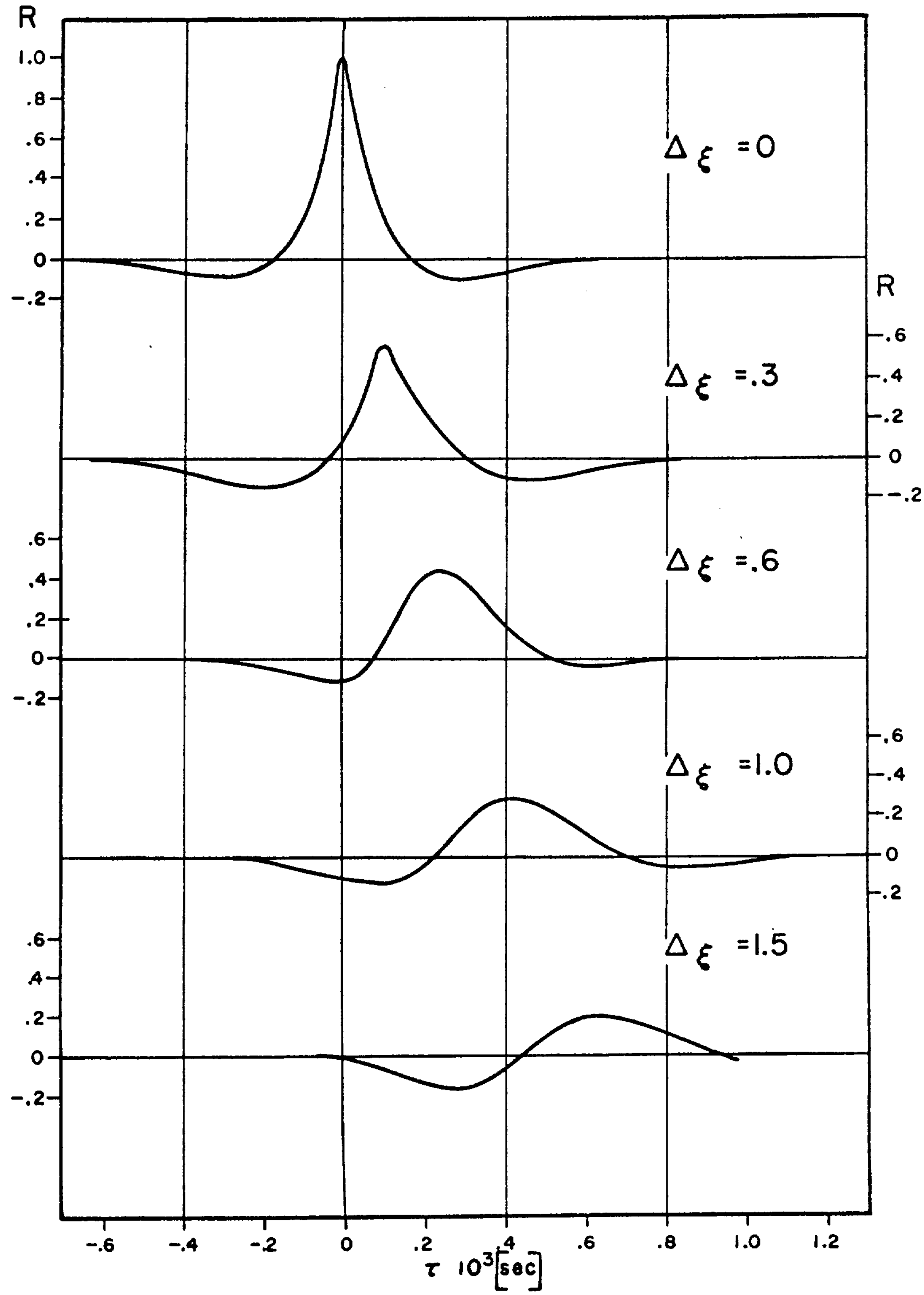

Figure 7 Space-time Correlation Coefficient
$\xi = 2$, $M_{ex} = .3$, $\eta = 0$, $d = 1"$

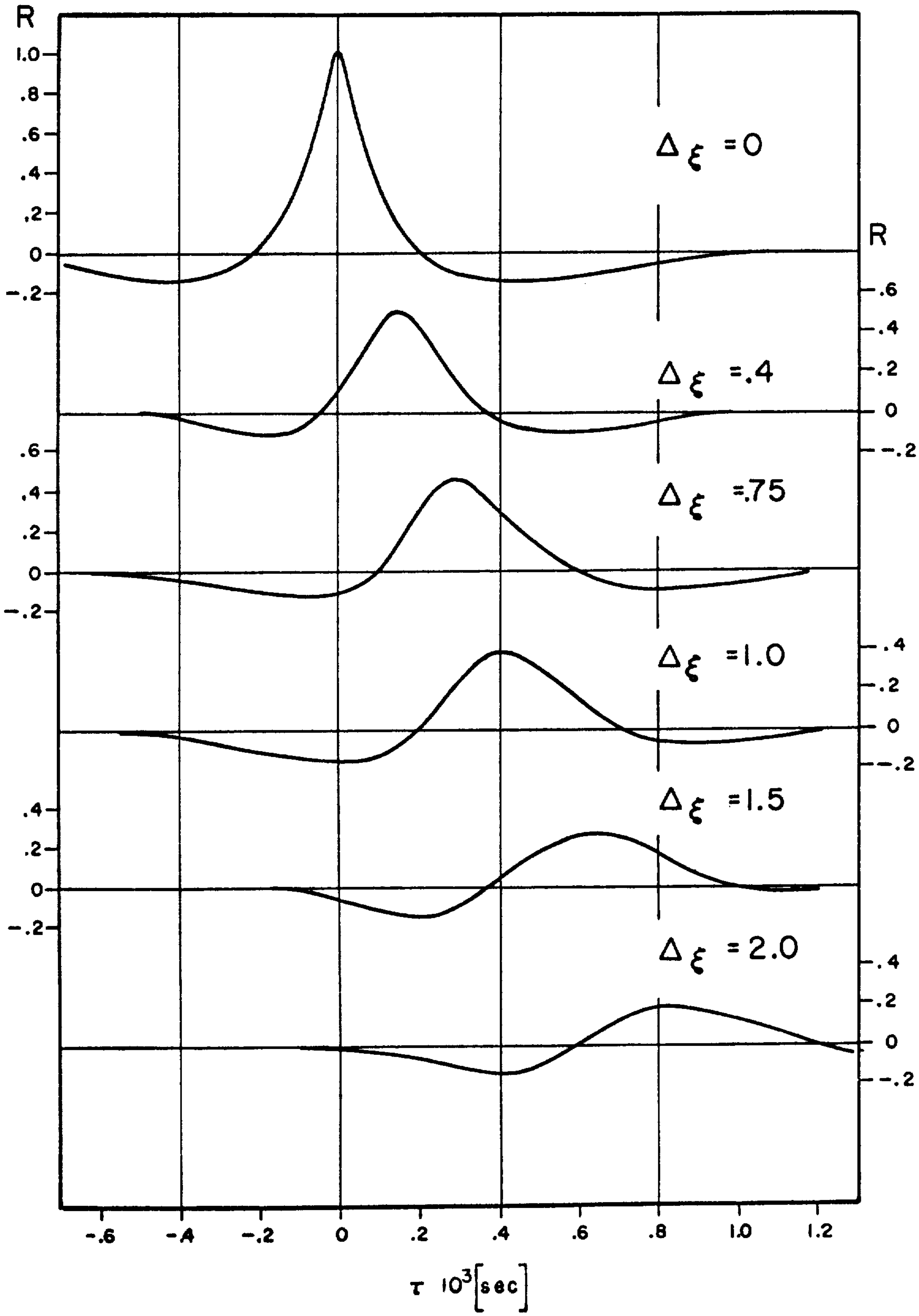

Figure 8 Space-time Correlation Coefficient.
$\xi = 3$, $M_{ex} = .3$, $\eta = 0$, d= 1"

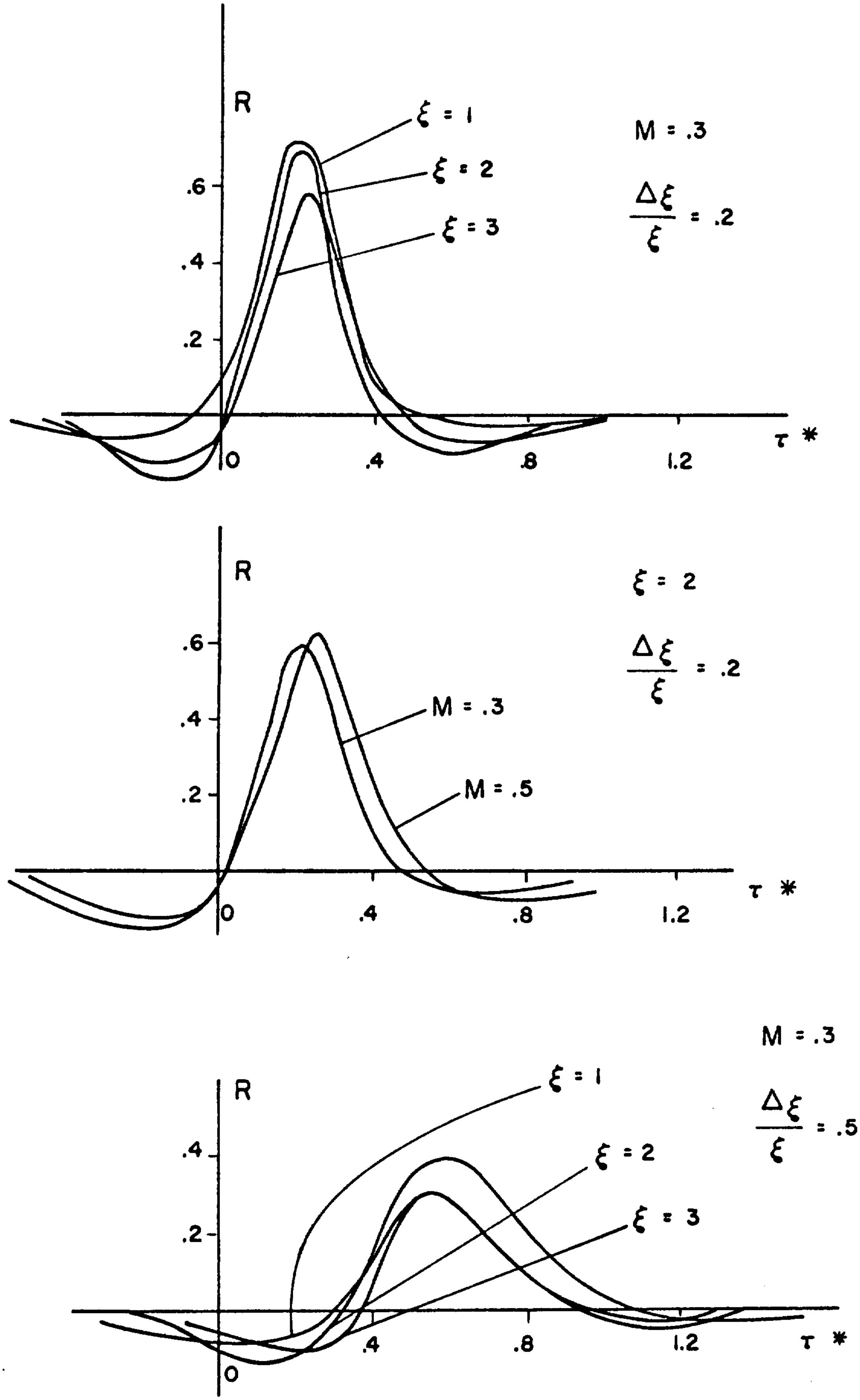

Figure 9. Similarity of the space-time correlation function.

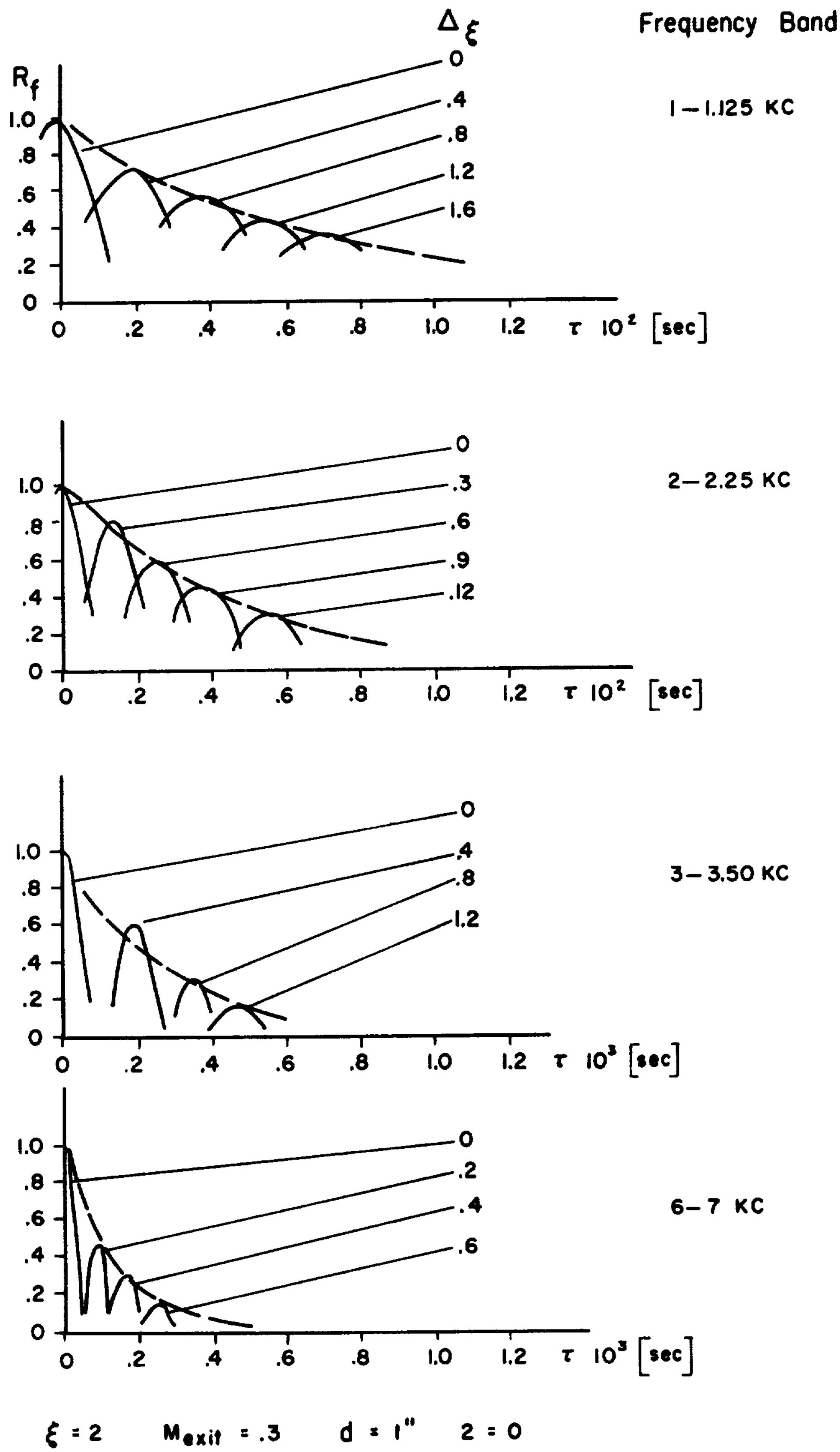

Figure 10. Space-time correlation for various frequency bands.

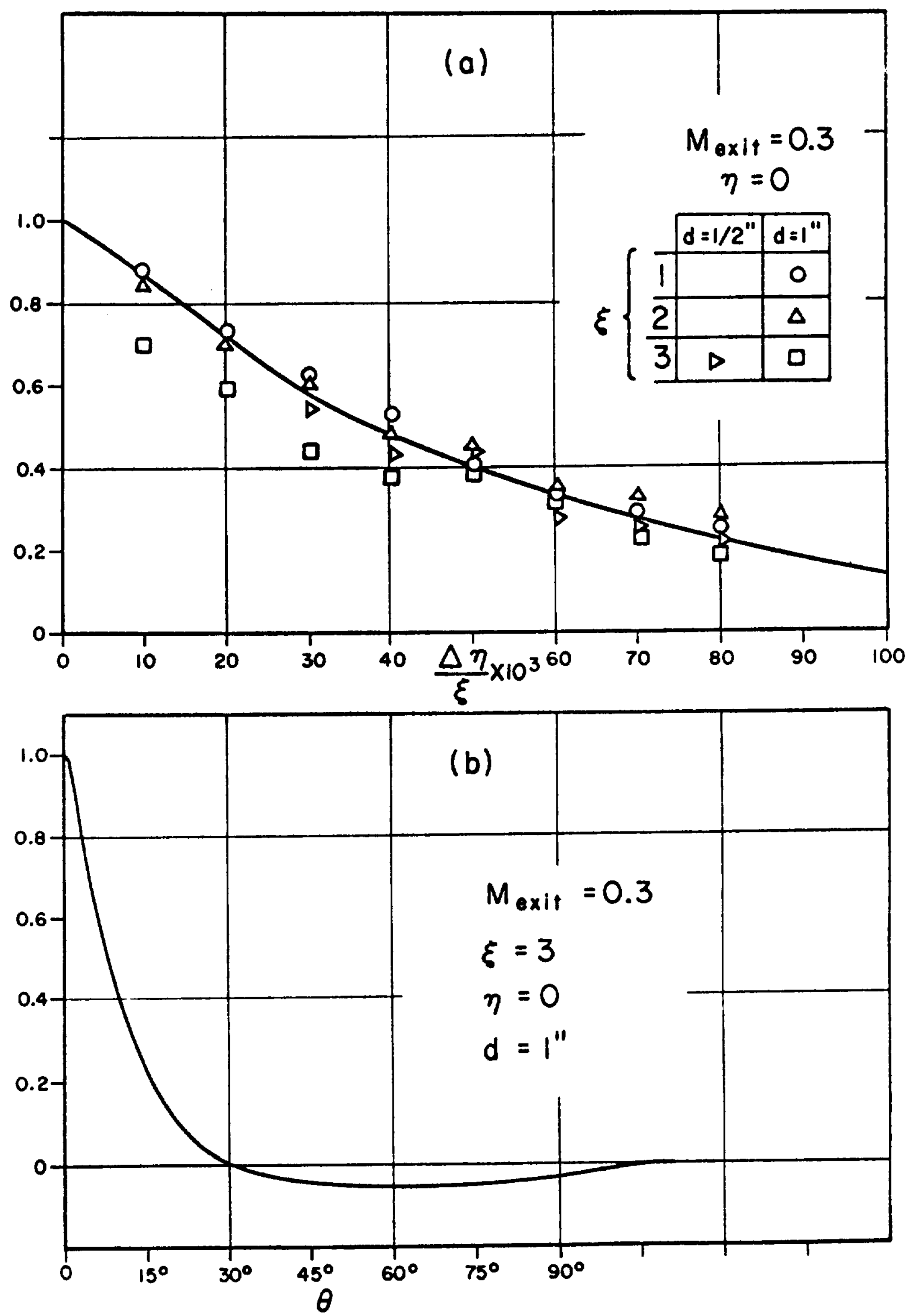

Figure 11 Lateral Correlation Coefficients.
(a) Wire Separation in Radial Direction
(b) Wire Separation in Angular Direction